Research Article

Journal of Environmental Nanotechnology

Synthesis of Environment-friendly Manganese-doped Metal Oxide Nanoparticles for the Biosensor Applications

M. Priyadharshini[1*], P. Rajesh[1], Syed Illiyas Syed Maqbool[1], V. Hariharan[2], M. Ezhil Inban[3]

[1]Department of Chemistry, Government Arts College, Coimbatore, TN, India
[2]Department of Physics, Mahendra Arts and Science College, Namakkal, TN, India
[3]Department of Physics, Government Arts College, Coimbatore, TN, India
Received: 21.07.2020 Accepted: 12.08.2021 Published: 30-09-2021
*dharshinimuthu93@gmail.com

ABSTRACT

The present work focuses on the synthesis of Manganese-doped Fe_2O_3 nanoparticles via an environment-friendly method that finds their suitability for biosensor applications using the extraction of Nyctanthes arbor-tristis seed for the first time. The synthesized Mn (~2, 3 & 5 wt. %) doped Fe2O3 were characterized by powder X-ray diffraction (XRD), Field emission Scanning electron microscopy (FE-SEM), Cyclic voltammeter (CV), Infrared and UV-Vis spectroscopic studies. The powder X-ray diffraction analysis exposed the phase formation and α-Fe_2O_3nanoparticles in the case of annealed sample. Also, interesting secondary phase formation was observed in the case of Mn (5 wt. %) doped samples. The optical properties of Mn (~2, 3 & 5 wt. %) doped Fe_2O_3 samples were determined by utilizing UV-Vis spectroscopic technique and the corresponding bandgap energy was found to be 5.52, 5.67 and 5.83 eV, respectively. The chemical bonds, as well as the functional groups in the compound, were confirmed by the analysis of the FT-IR spectrum. The morphology of the prepared samples was observed at the micro-level using FE-SEM analysis. A cyclic voltammeter was used to find the suit bio-sensorability of the prepared samples for proposed biosensor applications.

Keywords: Biosensor; Doped; Fe_2O_3; Manganese; Nyctanthes arbor-tristis

1. INTRODUCTION

In recent years, one of the hastily budding fields in science and technology is nanotechnology, bringing incredible development. The nanomaterial, which comprises typical physicochemical properties, has the prospective to thrive new systems, structures, devices, and nano-platforms with marked advances in boundless disciplines (Kalpana *et al.* 2018). Nanoparticle synthesis is decisive in understanding the particulate development process, modifying the nanoparticles' physicochemical properties and facilitating definite functionalities and applications. Mostly, nanoparticle synthesis methods can be characterized as top-down and bottom-up approaches. In the bottom-up approach, the building blocks utilized in synthesizing complex nanostructures are atoms and molecules. To fabricate needed nanostructures of disparate properties, the top-down approaches rely on the trimness of bulk particles. To establish nanoparticles' size, shape, and properties, both approaches are pertinent to the manufacturing of nanostructures for specific applications (Jeevanandam *et al.* 2016). Diverse varieties of nanoparticles, synthesized by unlike techniques, which possess altered properties, have found broad applications. They play distinct roles in different electrochemical and sensing systems. To immobilize bio-molecules, nanoparticles of metal oxides are used as a result of their biocompatibility. Owing to their unique magnetic, optical and electrical properties, Fe_2O_3 nanoparticles have gained massive attraction. NPs have been used in electrochemical biosensors due to their unique properties like huge surface area, high bioactivity, finest conformation stability and outstanding contact between biocatalyst and its substrate. Compared to general iron nanoparticles, magnetic nanoparticles are imperative in using biosensors. This is accredited to their small size and relatively large capacitance. Because of their diminutive size, such nanoparticles can effortlessly permit electrolyte ion transportation. Several physical and chemical methods are used to synthesize nanoparticles; however, several chemical procedures make use of toxic solvents which are not safe and generate hazardous by-products as well as habitually involve high energy consumption adopted in the synthesis of these NPs, which leads to toxicity in the environment (Rahman *et al.* 2017). Keeping this in mind, green technology by using plants is mounting as an eco-friendly, non-toxic and safe preference, while plant extract-mediated biosynthesis of nanoparticles offers natural capping agents in the form of proteins and is economically beneficial. Biological

synthesis of assorted metal oxide and metal nanoparticles through plant extraction is used to standardize chemical toxicity in the environment, which is a trivial technique for regulating chemical synthesis. It permits a discrete shape and size of nanoparticles with a detailed synthesis. Green synthesis of nanoparticles employs the bottom-up approach where the metal atoms accumulate to form clusters and ultimately the nanoparticles. To synthesize nanoparticles, various plant extracts derived from stem, leaf, root, latex and seeds were used. Plant extracts restrain a range of phytoconstituents that possess different functional groups. These functional groups perform as reducing agents for the fabrication of stable nanoparticles, not including the addition of any synthetic chemicals (Mishra *et al.* 2020).

Precisely, *Nyctanthes arbor-tristis* is a mythological plant that belongs to the 'Oleaceae' family and they have high medicinal values. It is considered one of the most useful conventional medicinal plants in India. It is considered an important plant that yields exclusive medicinal products and has industrial significance. It has multiple medicinal properties such as anti-helminthic, anti-pyretic, anti-inflammatory, anti-oxidant, hepatoprotective, anti-leishmaniasis, anti-viral, anti-fungal, anti-histaminic, anti-malarial and anti-bacterial. Further, it is used as a laxative, in rheumatism, skin ailments, and sedative. Range of plant parts like seeds, leaves, flowers, bark, and fruits have been investigated for their foremost pharmacological activity in addition to phytochemicals and publicized the presence of flavonoid, glycoside, oleanic acid, essential oils, tannic acid, carotene, fraudulent, lapel, glucose and benzoic acid recognized for a noteworthy hair tonic. Thus this non-toxic and benign seed extract is used to synthesize iron oxide nanoparticles (Hetal Bhalakiya and Nainesh, 2019).

To augment the potential applications of Fe_2O_3 nanostructures in biomedicine, they are being broadly investigated so far. The functionality and efficiency of Fe_2O_3 nanoparticles and nanostructures can be enhanced by increasing and modifying their surface area by adding some dopant materials, i.e., transition metals (Mn, Fe, Cr, and Cu) at the nanoscale. In surface modification with transition metals, Fe_2O_3 nanoparticles could be used as biosensors, antimicrobial, antioxidants, drug delivery systems and bio-imaging materials. Different methods have been developed for the production of Fe_2O_3 and transition metal-doped Fe_2O_3 nanoparticles (Khan *et al.* 2017). Essentially Fe_2O_3 can be tuned by particle size deviation and iron cation-replacement with divalent, trivalent and tetravalent cations having original spinel structure i.e., Mn^{2+}replace Fe^{3+} in tetrahedral AO_4 in doped Fe_2O_3 (Wahab *et al.* 2019).

By bearing in mind the significance of Fe_2O_3 nanoparticles, the current work focuses on the green synthesis of Mn-doped Fe_2O_3 nanoparticles for biosensor application using the extract of *Nyctanthes arbor-tristis* seed for the first time.

2. EXPERIMENTAL SECTION

2.1 Materials and Preparation Methods

The precursors such as $FeCl_3$ and NH_3 (analytical grade) were purchased from Merc and used as such without any additional purification. The extraction of *Nyctanthes arbor-tristis* was carried out using de-ionized water. The mixture of iron solution with the extraction of *Nyctanthes arbor-tristis* was kept under the stirring process in order to acquire immaculate iron hydroxide using the chemical precipitation method. Aqueous ammonia solution was added dropwise to maintain the pH of the solution. To the above solution, the manganese (~ 2, 3 & 5 wt. %) solution was added dropwise using a burette, which acted as a dopant and kept again for the stirring process. Further, the supernatant solution was removed and washed several times to remove chlorine ions. The obtained powder was dried using a hot plate and kept in muffle furnace at 600°C/air/6h to remove the impurities and improve the crystallinity.

2.2 Characterization Methods

To swot the physicochemical properties, the synthesized samples are categorized methodically. By means of BRUKER D8 ADVANCED X-ray Diffractometer in Bragg-Brentano geometry, the structure and crystallinity of the samples are inveterate via Cu K-alpha radiation (λ=1.5406 Å). By using FE-SEM (HITACHI S-3400), the Surface morphology of the synthesized composites was studied. Charge-discharge method and the electrochemical performance of cyclic voltammeter (CV) were carried out by means of CHI 604C potentiostat in a three-electrode assemblage.

3. RESULTS AND DISCUSSION

3.1 Powder XRD Analysis

X-ray diffraction pattern was used to cram the crystal structure of Mn-doped Fe_2O_3 (~2, 3 & 5 wt. %) samples (Fig. 1). The 2 wt. % Mn-doped Fe_2O_3 sample shows the high intense diffraction peak in the order of $2\theta = 33^{o}.7'$, which is well-reliable with a rhombohedrally-centered hexagonal Fe_2O_3 with space groups R3c (JCPDS No. 33-0664). It was detected that it does not show any peaks of manganese oxide. The development of a homogeneous Mn-Fe-O solid solution established the high purity of the sample. Owing to the preamble of manganese there is a steady decrease of peak intensity and trivial narrowing of the peak width occurs which indicates that the Mn oxides were in a highly disseminated state. Moreover, the grain size of Mn-doped Fe_2O_3 was smaller compared to pure Fe_2O_3 which was

confirmed by the fact that the full width at half maximum of the peaks for Mn-doped Fe_2O_3 were lower compared to Fe_2O_3. This indicated that the crystallinity of Fe_2O_3 was lowered by the survival of Mn ions which could augment the dispersion of Fe_2O_3 on the catalyst surface. The corresponding average crystallite size calculated from the Debye-Scherrer equation for 2 wt. % Mn-doped Fe_2O_3 sample was established to be 10.34 nm (Zhao *et al.* 2016). In the case of Mn (~3 & 5 wt. %) doped Fe_2O_3 sample, the high intense diffraction peak occurs around $2\theta = 50^{o}.4'$and $44^{o}.3'$. This is owing to the development of secondary crystallite phase that attributable to any other oxidation state of iron, which confirms that the (~3 & 5 wt. %) Mn-doped Fe_2O_3 samples have several impurities otherwise there is a possibility of a shift in the peak when the concentration of manganese increases in the sample. The corresponding average crystallite sizes for the above samples were calculated as 61 nm and 22 nm, respectively, by using the Debye-Scherrer equation (Xu *et al.* 2015).

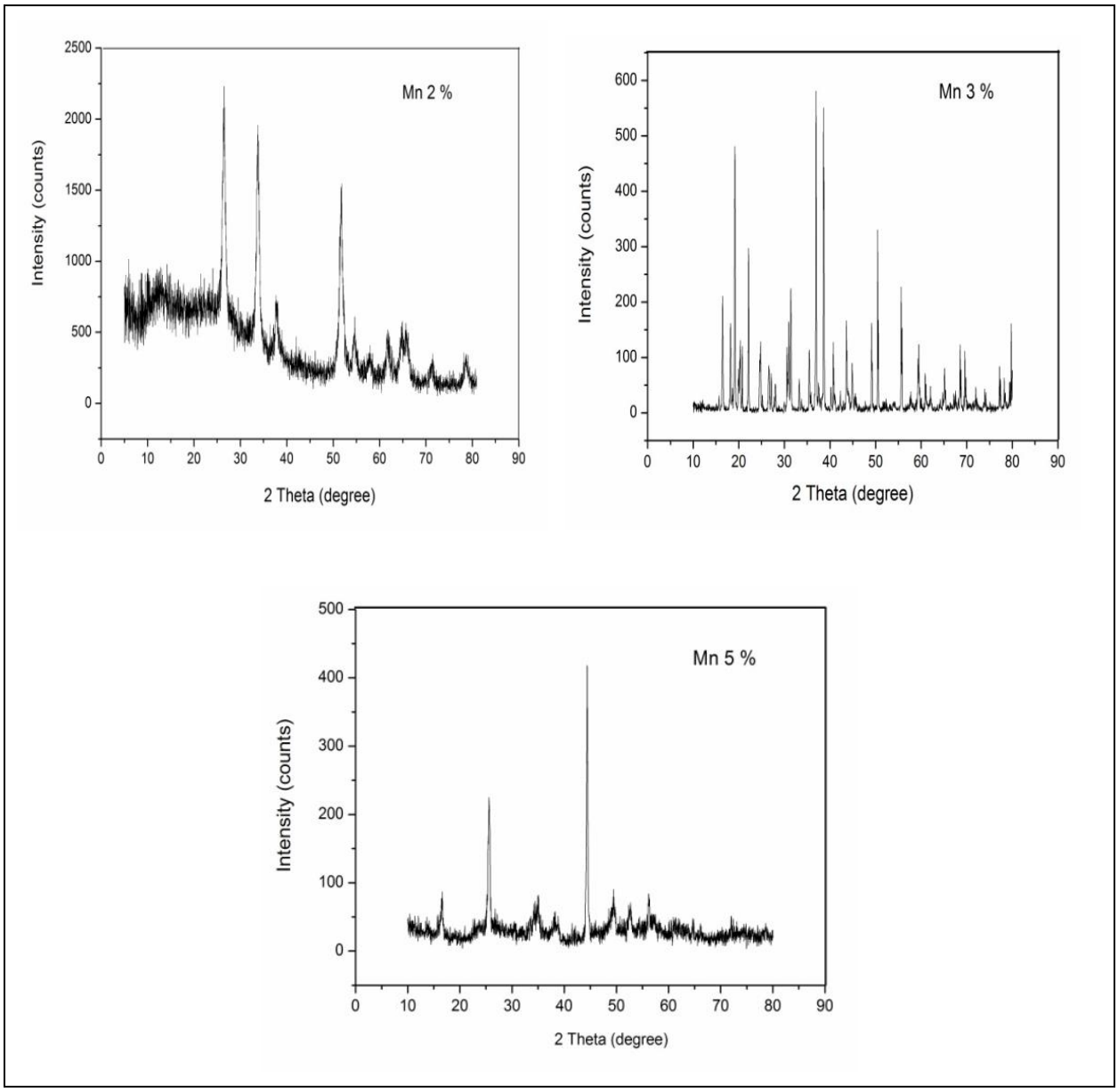

Fig. 1: Powder XRD pattern of Mn (~2, 3 & 5 wt. %) doped Fe_2O_3 nanoparticles

3.2 UV-Visible Spectroscopic Analysis

UV-Vis spectroscopic technique was used to determine the optical properties of Mn (~2, 3 & 5 wt. %) doped Fe_2O_3 samples. They show a shift towards the blue region, as shown in Fig. 2, and also, the obtained absorption edge may be corresponding to α-Fe_2O_3 nanoparticles. The shift towards the lower wavelength (blue shift region) is in agreement with Powder XRD analysis due to the crystalline nature of the synthesized materials, which was confirmed by the corresponding optical absorption peak arising at 212 nm.

The extraction from *Nyctanthes arbor-tristis* plant does not give rise to any other absorption peaks. Using Tauc plot, the energy bandgap values for Mn (~2, 3 & 5 wt. %) doped Fe_2O_3 nanoparticles after annealing was found to be 5.52, 5.67 and 5.83 eV, respectively. In association with the reduction of the bandgap energy, the absorption curve had shifted towards the blue region and the reason behind this was explained by the Tauc plot. It also explains the recombination rate, which may lead to the photovoltaic activity applications of the prepared samples (Piccinin *et al.* 2019).

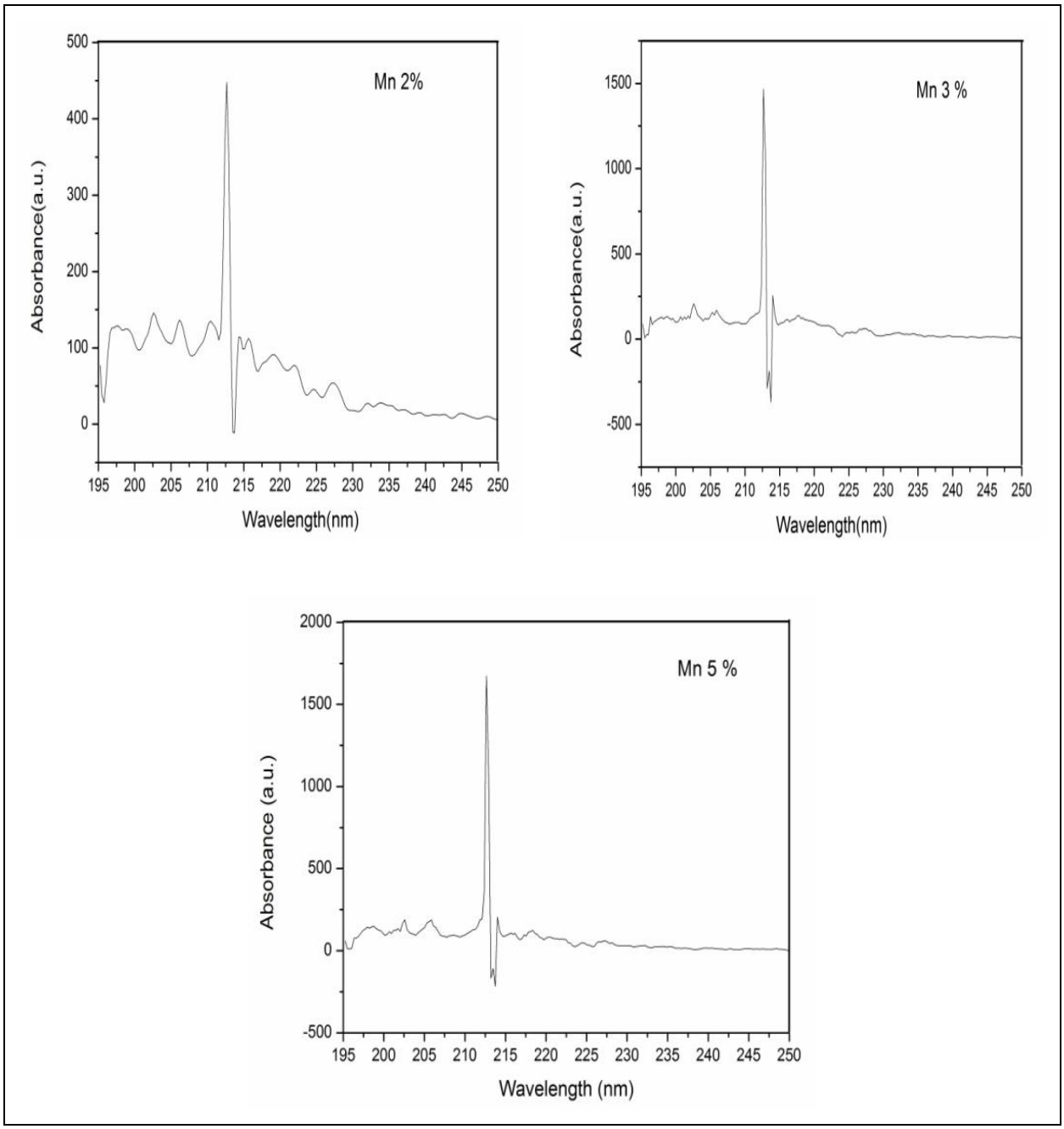

Fig. 2: UV-Visible absorption spectrum of Mn (~2, 3 & 5 wt. %) doped Fe_2O_3 nanoparticles

3.3 FT-IR Analysis

According to Fig. 3, the infrared spectrum (FT-IR) of the synthesized Fe_2O_3 nanoparticles was 400-4000 cm^{-1} wave number, which identifies the chemical bonds and functional groups in the compound. The FTIR spectra reveal that the stretching vibrations in the regions between 3175 to 3726 cm^{-1} belong to -NH stretching and alkyl stretching vibrations, respectively, confirming the trace of extraction of the plants during the synthesis process. The large broadband at 3398 cm^{-1} can be ascribed to the O-H stretching vibration in OH^- groups. The absorption peaks around 1604 cm^{-1} and 1487 cm^{-1} are due to the asymmetric and symmetric bending vibration of C=O. The strong band below 700 cm^{-1} can be assigned to the Fe-O stretching mode. The band corresponding to Fe-O stretching mode of Fe_2O_3 is seen at 576 cm^{-1} (Majid Farahmandjou *et al.* 2015).

3.4 FE-SEM Analysis

The microscopic (FE – SEM) nature of the doped Fe_2O_3 prepared samples is shown in Fig. 4. It reveals that the samples were not fully resolved due to the formation of α-Fe_2O_3 in association with plant extraction to low calcination temperature. The morphology of the prepared samples was found to be aggregated spherical shape in nature with the dimension in the order of 6 to 8 μm. In addition, it clearly shows the role of dopant and extraction during the synthesis of α – Fe_2O_3 nanoparticles in the case of both as-prepared and annealed samples.

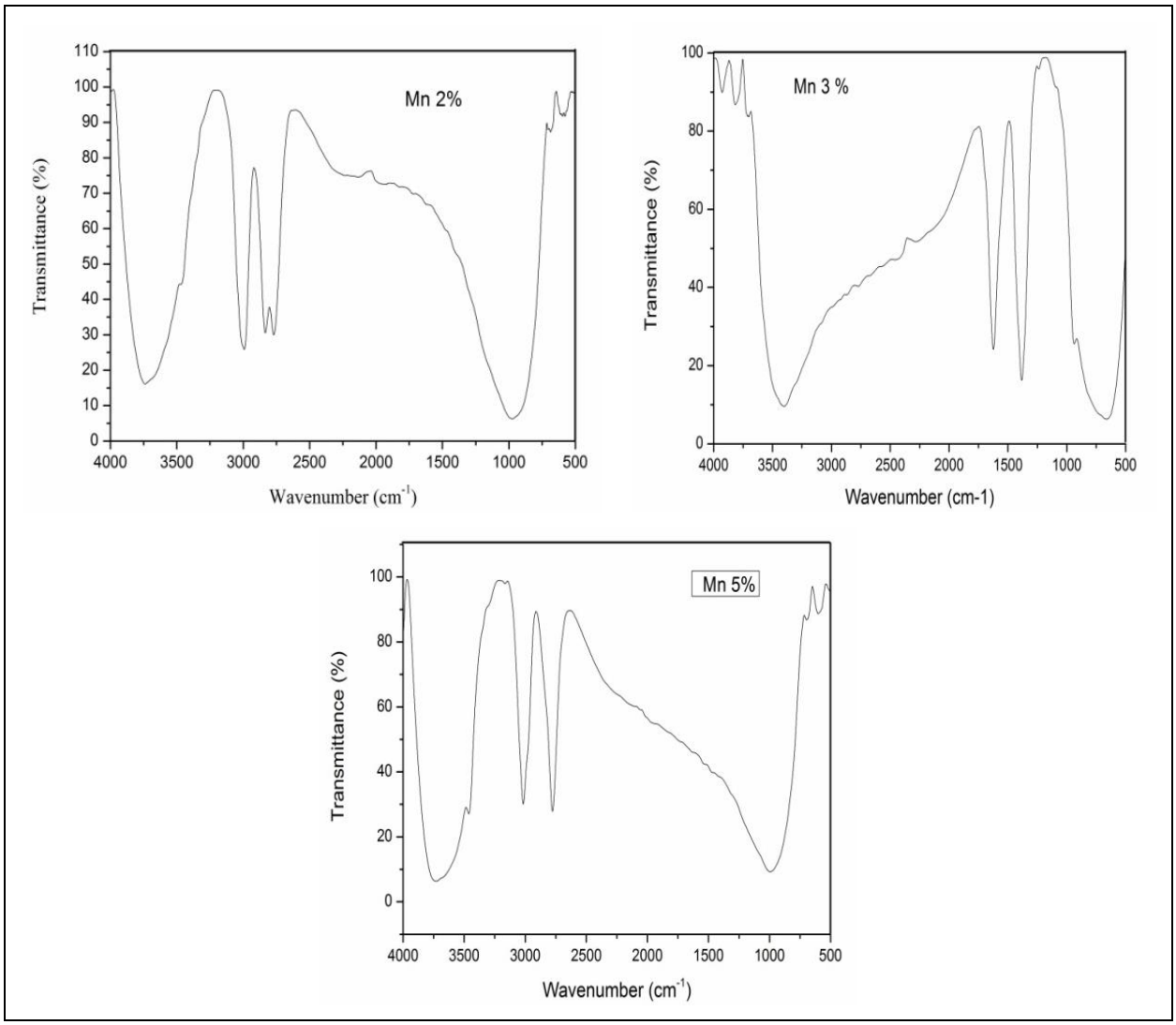

Fig. 3: FT – IR spectra for α-Fe_2O_3 nanoparticles

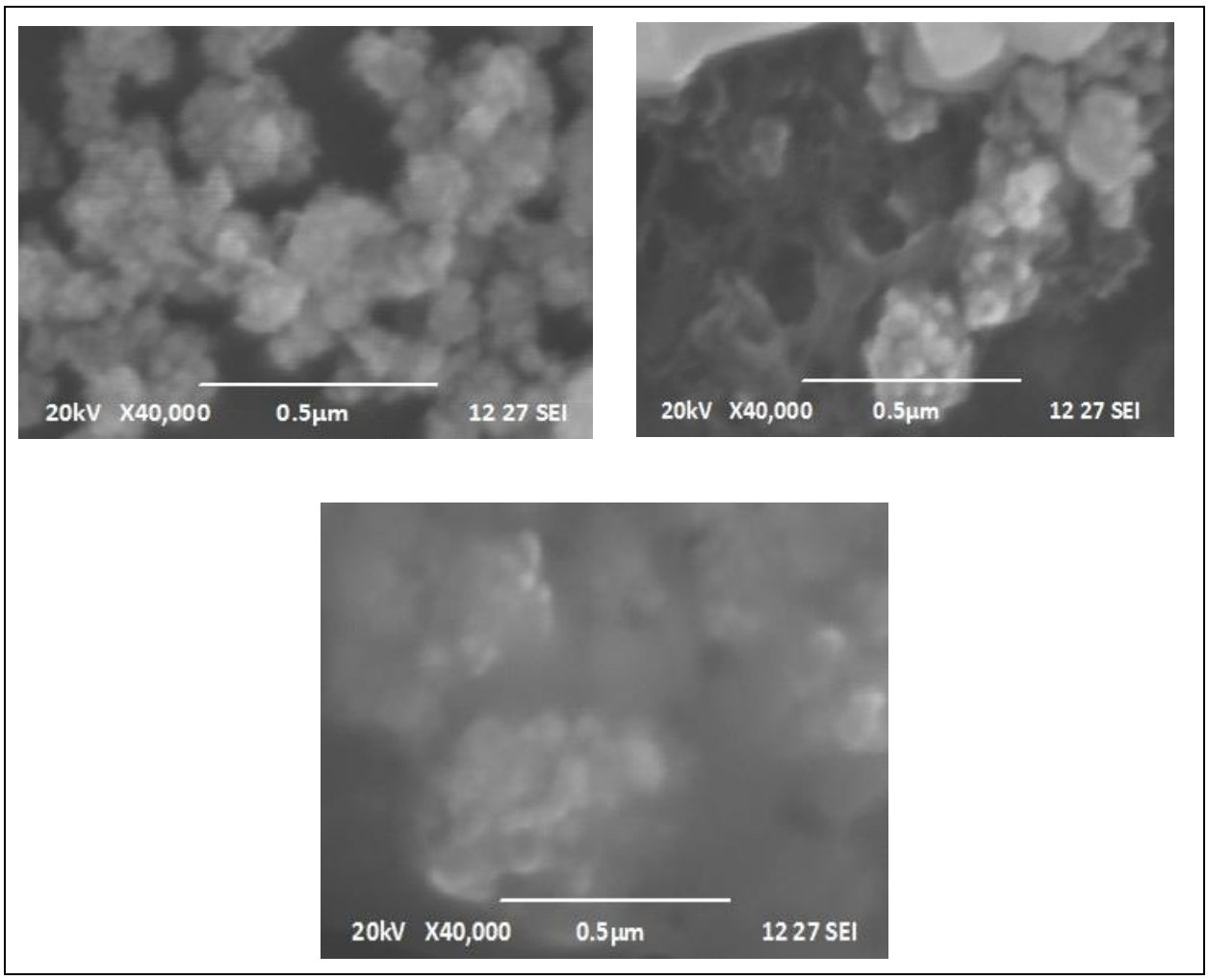

Fig. 4: FE-SEM Spectra of Mn (~2, 3 & 5 wt. %) doped Fe_2O_3 nanoparticles

3.5 Electrochemical Analysis

In order to find the suitability of the annealed pure and doped α-Fe_2O_3 nanoparticles for biosensor applications, Cyclic voltammetry (CV) study was performed in the voltage window range from 0 to 1 V using a three-electrode system in 1 M aqueous solution of $FeSO_4$ and chitosan-based electrolyte solution. The respective CV curves of the various electrodes recorded with the sweep rates of 10, 20, 40, 60, mVs^{-1} at room temperature are illustrated in Fig. 5. The obtained single oxidation as well as reduction potential due to Mn 5 wt.% doped annealed α-Fe_2O_3 nanoparticles shows excellent sensing behavior, as evident from Fig. 5. The lower scan rate, the CV curves of the α-Fe_2O_3 nanoparticle-based electrode exhibit redox peaks attributable to the reversible Faradaic redox reaction at the electrode surface caused by the pseudo-capacitance of the α-Fe_2O_3 nanoparticles as an active material, rather than the double-layer capacitance. Also, it is to be observed that nature reveals the linear progress CV curves during high scan rates with the current response to voltage reverse at each potential.

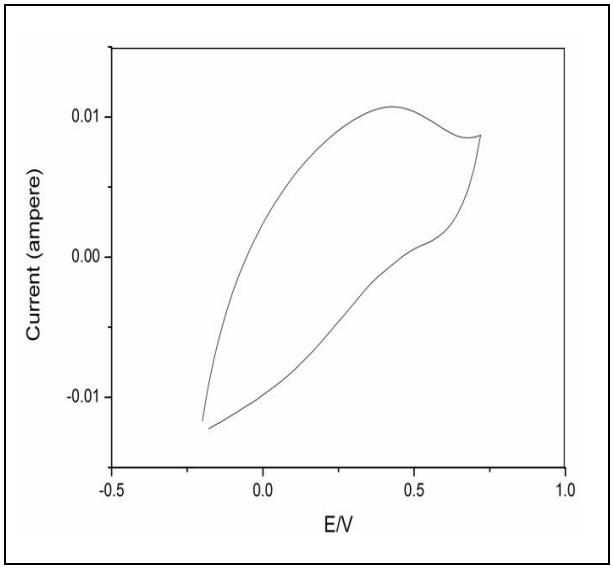

Fig. 5: Electrochemical performance of annealed Mn-doped iron oxide (Fe_2O_3) nanoparticles

4. CONCLUSION

By adopting an eco-friendly preparation technique, Mn (~2, 3 & 5 wt. %) doped Fe_2O_3 samples were synthesized with reduced size and comparatively large capacitance via *Nyctanthes arbor-tristis* seed extract. The synthesized doped samples have dimensions of the order of 6 to 8 μm which is in agreement with the Powder XRD analysis of both as-prepared and annealed samples. The bandgap energy was found to be 5.83 eV by Tauc plot that established the optical nature of the synthesized compound, having a good concord with the Powder XRD. The electrochemical analysis exposed the excellent sensing behavior of the Mn-doped Fe_2O_3 nanoparticles, which display redox peaks attributed to the reversible Faradaic redox reaction at the electrode surface was caused by the pseudo-capacitance of the α-Fe_2O_3 nanoparticles as an active material than the double-layer capacitance. Consequently, the current work demonstrates a novel scheme and design for a better sensing biosensor based on Mn-doped Fe_2O_3 nanoparticles synthesized by an effortless and cost-effective green synthesis method.

FUNDING

This research received no specific grant from any funding agency in the public, commercial, or not-for-profit sectors.

CONFLICTS OF INTEREST

The authors declare that there is no conflict of interest.

REFERENCES

Hetal Bhalakiya and Nainesh R. Modi, Traditional medicinal uses, phytochemical profile and pharmacological activities of Nyctanthes Arbortris, 5(2), 1003-1023 (2019). https://dx.doi.org/10.26479/2019.0502.76

Jeevanandam, J., Chan, Y. S. and Danquah, M. K., Biosynthesis of metal and metal oxide nanoparticles, *Chem. Bio. Eng. Rev.*, 3(2), 55–67 (2016). https://dx.doi.org/10.1002/cben.201500018

Kalpana, V. N. and Devi Rajeswari, V., A Review on green synthesis, biomedical applications, and toxicity studies of ZnO NPs, *Bioinorg. Chem. Appl.*, 2018, 1–12 (2018). https://dx.doi.org/10.1155/2018/3569758

Khan, S. A., Shahid, S., Bashir, W., Kanwal, S. and Iqbal, A., Synthesis, characterization and evaluation of biological activities of manganese-doped zinc oxide nanoparticles, *Trop. J. Pharm. Res.*, 16(10), 2331–2339 (2017). https://dx.doi.org/10.4314/tjpr.v16i10.4

Majid Farahmandjou and Soflaee, F., Synthesis and characterization of α-Fe_2O_3 nanoparticles by simple co-precipitation method, *Phys. Chem. Res.*, 3(3), 191–196 (2015). https://dx.doi.org/10.22036/pcr.2015.9193

Mishra, A. K., Tiwari, K. N., Saini, R., Kumar, P., Mishra, S. K., Yadav, V. B. and Nath, G., Green synthesis of silver nanoparticles from leaf extract of *Nyctanthes arbor-tristis* L. and assessment of its antioxidant, antimicrobial response, *J. Inorg. Organomet. Polym. Mater.*, 30(6), 2266–2278 (2020). https://dx.doi.org/10.1007/s10904-019-01392-w

Piccinin, S., The band structure and optical absorption of hematite (α-Fe_2O_3): A first-principles GW-BSE study, *Phys. Chem. Chem. Phys.*, 21(6), 2957–2967 (2019). https://dx.doi.org/10.1039/C8CP07132B

Rahman, S. S. U., Qureshi, M. T., Sultana, K., Rehman, W., Khan, M. Y., Asif, M. H., Farooq, M. and Sultana, N., Single-step growth of iron oxide nanoparticles and their use as glucose biosensor, *Results Phys.*, 7, 4451–4456 (2017). https://dx.doi.org/10.1016/j.rinp.2017.11.001

Wahab, A., Imran, M., Ikram, M., Naz, M., Aqeel, M., Rafiq, A., Majeed, H. and Ali, S., Dye degradation property of cobalt and manganese doped iron oxide nanoparticles, *Appl. Nanosci.*, 9(8), 1823–1832 (2019). https://dx.doi.org/10-1007/S13204-019-00970-1

Xu, S., Habib, A. H., Gee, S. H., Hong, Y. K. and McHenry, M. E., Spin orientation, structure, morphology, and magnetic properties of hematite nanoparticles, *J. Appl. Phys.*, 117(17), 17A315 (2015). https://dx.doi.org/10.1063/1.4914059

Zhao, G., Li, J., Niu, X., Tang, K., Wang, S., Zhu, W., Ma, X., Ru, M., Yang, Y., Facile synthesis of Mn-doped Fe_2O_3 nanostructures: enhanced CO catalytic performance induced by manganese doping, *New J. Chem.*, 40(4), 3491–3498 (2016). https://dx.doi.org/10.1039/C5NJ0369